Detection of Multiple Active Site Domain Motions in Transient-State Component Time Courses of the *Clostridium symbiosum* L-Glutamate Dehydrogenase-Catalyzed Oxidative Deamination Reaction†

Jon F. Tally, Steven J. Maniscalco, Swapan K. Saha, and Harvey F. Fisher*

Laboratory of Molecular Biochemistry, Veteran Affairs Medical Center, and Department of Biochemistry, University of Kansas Medical Center, Kansas City, Missouri 64128

Received March 14, 2002; Revised Manuscript Received July 11, 2002

ABSTRACT: We present a multiwavelength, transient-state kinetic study of the oxidative deamination reaction catalyzed by *Clostridium symbiosum* glutamate dehydrogenase (csGDH) producing the real-time reaction courses of spectroscopically resolved kinetically competent intermediate complexes. The results show striking differences from a corresponding transient-state study of the same reaction by the structurally homologous enzyme from beef liver (blGDH). In addition to the highly blue-shifted α-iminoglutarate and highly red-shifted carbinolamine complexes observed in both reactions, the csGDH reaction appeared to show the release of free NADH at a very early and mechanistically unlikely point in the reaction. Using lactic acid dehydrogenase as a "reporter" for free NADH, we show that the early portion of this signal reflects previously unobserved spectrally unshifted enzyme-bound NADH complexes. We provide experimental evidence to show that such spectrally anomalous complexes must represent forms of the known α-imino and α-carbinolamine complexes in which the active site cleft is open. This evidence includes isothermal calorimetric measurements and pH-jump experiments that show the existence of differing two-state transitions in blGDH and csGDH and locate active site domain motions at differing points in the transient-state time courses of the two enzyme reactions. We prove the kinetic competence of a new and more highly detailed mechanism for the csGDH reaction that involves the alternation of open and closed enzyme complexes as integral steps. These findings, supported by the available X-ray crystal structure data, suggest the existence of a programmed time course of protein domain motions coordinated with the classically considered chemical time course. This new viewpoint may be presumed to be applicable to enzyme reactions other than those of the α-amino acid dehydrogenases.

L-Glutamate dehydrogenases form a subclass of the pyridine nucleotide linked L-α-amino acid dehydrogenases (*1*). Members of this group of enzymes all catalyze reactions having the stoichiometry

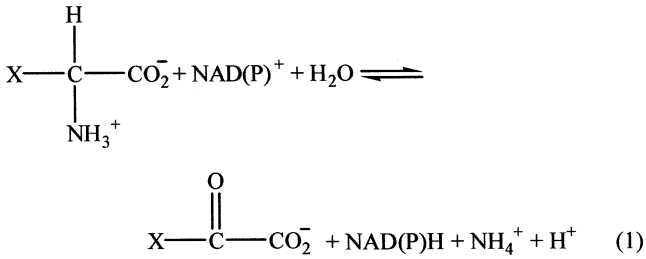

(1)

where X represents the specific amino acid residue. On the basis of steady-state kinetics and chemical intuition (*2*), it has been generally assumed that the reactions catalyzed by this class of enzymes proceed through a mechanism involving the following sequence of bound substrate intermediates:

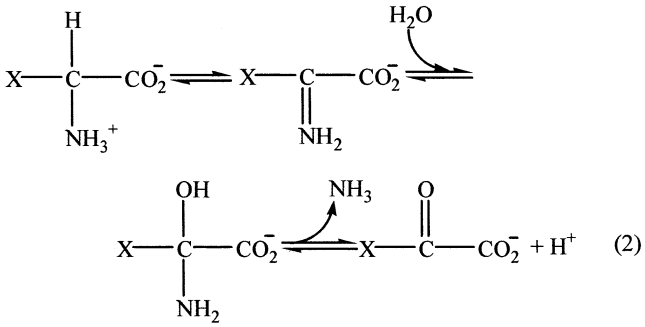

(2)

This mechanism, originally suggested by Rife and Cleland (*2*) for the bovine liver glutamate dehydrogenase (blGDH)[1] reaction, predicted that an enzyme carboxylate group removes a proton from the substrate α-amino acid group prior to hydride transfer and that an enzyme ϵ-amino group must

† This work was supported in part by the Department of Veterans Affairs and by Grant MCB-9513398 from the National Science Foundation.

* Address correspondence to this author at Research Service, VA Medical Center, 4801 Linwood Blvd., Kansas City, MO 64128. Telephone: (816) 861-4700, ext 7156. Fax: (816) 861-1110. E-mail: hfisher@kumc.edu.

[1] Abbreviations: csGDH, *Clostridium symbiosum* glutamate dehydrogenase; blGDH, bovine liver glutamate dehydrogenase; E, enzyme; O, oxidized coenzyme (NAD or NADP); R, reduced coenzyme (NADH or NADPH); I, α-iminoglutarate; C, α-carbinolamine; K, α-ketoglutarate; N, ammonia.

10.1021/bi0202068 CCC: $22.00
Published on Web 08/22/2002

hold a water molecule in a position suitable for a nucleophilic attack on the α-amino carbon atom to form a carbinolamine. This prescient prediction was strongly supported by the crystallographic structures of *Clostridium symbiosum* glutamate dehydrogenase (csGDH) by Rice and Engel and their collaborators (*3*, *4*), which indeed showed an aspartyl residue and a water molecule bound to a lysyl nitrogen atom in the precise positions predicted.

While these inferences from steady-state kinetic studies and crystal structures of necessarily static enzyme complexes are consistent with the mechanism shown in eq 2, they cannot provide the direct evidence required to prove the existence of the postulated reactive amino acid (EOG′), α-imino acid (ERI), α-carbinolamine (ERC), and α-keto acid (ERK) complexes nor are they suitable for the task of evaluating their physical properties and exploring the nature of their interconversion steps. To provide this needed information, we have developed and used a transient-state multiwavelength spectroscopic approach that has provided direct evidence of occurrence and subsequent conversion in real time of each of these postulated entities and established their kinetic competence in the reaction described in eq 2 (*5*). The individual species, characterized by the direction and magnitude of the shifts of their spectra from the λ_{max} of 340 nm of free NAD(P)H, included an ultra-blue-shifted ER−α-iminoglutarate complex ERI ($\lambda_{max} = 327$ nm), an ultra-red-shifted α-carbinolamine species, ERC ($\lambda_{max} = 349$ nm), and a blue-shifted ER−α-ketoglutarate complex ERK ($\lambda_{max} = 333$ nm). A weakly absorbing but highly fluorescent red-shifted EO−L-glutamate charge-transfer complex, EOG′, was also identified (*6*). Corresponding species (with minor differences in λ_{max}) have been observed in csGDH and phenylalanine dehydrogenase systems. It is curious to note that, in all complexes of enzymes of this class, the spectra are invariably red shifted to some degree where the α-carbon atom of the ligand is tetrahedral (sp^3), and they are blue shifted in all cases where the ligand α-carbon atom is in a C═O or C═N (sp^2) form. X-ray crystallographic structures of at least seven α-amino acid dehydrogenases have shown that at least a dozen conserved enzyme functional groups are located at the active sites of all of these enzymes, occupying nearly identical positions. On this basis, it was reasonably assumed that the enzymes of this class all followed the same detailed mechanism. This assumption appears to remain true in a general way. However, some recent observations have suggested that there may be very significant variations in the precise manner in which each member of this class carries out the specific steps of the overall common mechanism. First of all, we have shown that while the proton is released in a *pre*hydride transfer step in the blGDH reaction, it is released in a *post*hydride transfer step in the csGDH reaction (*7*). Further, Brunhuber et al. have concluded from their structural studies that, unlike the csGDH reaction where an aspartyl carboxylate oxygen appears to abstract a hydrogen atom from the bound substrate α-amino group, in the PaDH reaction this carboxylate oxygen atom is too far away to accomplish this task. Instead, the hydrogen atom is transferred to the nearby lysyl nitrogen atom through its bound water molecule that serves as a bridging atom (*8*). Finally, preliminary transient-state studies from our laboratory have shown that the resolved spectroscopic component time courses of the three enzymes showed distinctively different phenomenological patterns despite their rather similar steady-state kinetic behavior.[2] Here, we present our analysis of the complex formation and interconversion phenomena in the csGDH reaction and compare the results with the corresponding but very different phenomena of the blGDH reaction.

MATERIALS AND METHODS

Materials. *C. symbiosum* glutamate dehydrogenase (csGDH) was prepared from an *Escherichia coli* PA340 (PTAC44) clone and kindly given to us by X. G. Wang. Purification of this enzyme from the IPTG (isopropyl β-D-thiogalactopyranoside) induced csGDH gene in the *E. coli* clone was done by the Remazol dye column method of Rice et al. (*9*). After column purification the specific activity was verified by assay at 25 °C using 40 mM L-glutamate and 1 mM NAD in 0.1 M potassium phosphate buffer, pH 7.0. Pig heart H4 lactate dehydrogenase (LDH) in a 2 M ammonium sulfate suspension was purchased from Roche Biochemical. Stock enzyme was dialyzed against three changes of 0.1 M potassium phosphate buffer at the required pH and at 4 °C. LDH enzyme activity was verified by assay in 0.1 M potassium phosphate buffer, pH 7.4, containing 10 mM pyruvate and 66 μM NADH at 25 °C. Prior to use, GDH preparations were centrifuged at 1500 rpm and filtered through approximately 1 mg/mL Norit A on a 0.45 μm Millipore filter. Enzyme concentrations were measured spectroscopically at 280 nm using an $\epsilon = 54.4$ cm^{-1} mM^{-1} for blGDH, $\epsilon = 51.6$ cm^{-1} mM^{-1} for csGDH, and $\epsilon = 49.7$ cm^{-1} mM^{-1} for LDH. NAD and L-glutamate were purchased from Sigma and were used without further purification.

General Methods. All experiments involving csGDH reported here, except where otherwise noted, were carried out in 0.1 M phosphate buffer at 5 °C. Transient-state kinetic measurements and the resolution of intermediate components were done as described earlier (*5*). Absorbance versus wavelength and time matrix arrays were constructed using an Applied Photophysics SX-17MV stopped-flow spectrophotometer equipped with a sequential mixing accessory. The reaction was carried out at 5 °C in 0.1 M phosphate buffer, pH 7.0, 45 mM L-glutamate, 380 μM NAD, and 45 μM enzyme.

Determination of Model Spectra. Spectra of stable complexes of csGDH were determined by an approach previously developed and used to define and characterize those of the corresponding complexes of blGDH. The spectra of the E−NADPH, E−NADH, E−NADPH−L-glutamate, E−NADPH−α-ketoglutarate, E−NMNH, E−deamino NADH, E−acetylpyridine NADH, and E−ADP complexes were described in a 1972 review (*10*). A detailed description of the modified version of that approach used here to obtain the model spectra required for the resolution of csGDH transient-state multiwavelength absorbance arrays has been described in ref *11*. Briefly, it involves the following steps: A set of difference spectra of the general form (E, A, B, C) − (E + A + B + C) are obtained in an HP 8450 multidiode spectrophotometer

[2] We have speculated elsewhere (*23*) that differences in the patterns of hydrogen bonding of a highly conserved atomic tetrad in the active site of α-amino acid dehydrogenases may play some part in the qualitative differences observed in the transient-state time courses of these enzymes.

at varying concentrations of NADH. A single well-defined difference spectrum of this set representing a moderate degree of enzyme saturation is selected as a model. (This choice is not critical.) The rest of the set of difference spectra are then each matched against this model by using the multicomponent analysis algorithm built into the HP 8450. The results of these analyses obtained at varying values of [R] are then used to calculate the K_D of the given complex using the quadratic equation:

$$c/b = (R_T + E_T + K_D) - \sqrt{(R_T + E_T + K_D)^2 - 4R_T E_T} \quad (3)$$

Using this experimentally determined K_D, the concentration of bound R is calculated, and a spectral component corresponding to that amount of bound R is added to the model difference spectrum to generate the spectrum of the complex.

Resolution of Fixed-Time Transient Spectra. The set of procedures used to resolve individual fixed-time spectra has been described in detail in ref *5* where its success in showing the existence and occurrence along the time course of the transient blGDH−NADPH−α-iminoglutarate and blGDH−NADPH−α-carbinolamine complexes has been demonstrated. Here, we provide a brief description of the sequence of steps used to provide such resolutions. These steps are as follows: (1) the resolution of each fixed-time spectrum by a least mean squares process using an iterative Beer's law summation of the spectra of the stable entities was obtained as described above (ER, ERG, ERK, and R); (2) the correction of the experimental spectra for the small effect of the loss of oxidized coenzyme was as calculated from the observed total concentration of reduced coenzyme species; (3) the analysis of the residual spectrum representing the difference between the experimental spectrum and that of the initial resolution was performed; (4) based on the wavelength-dependent trends in that residual spectrum, putative transient-state model spectral components are added to the initial resolved component spectrum, and the least-squares analysis and subsequent correction for loss of NAD is carried out (models that produce negative components are rejected as physically impossible given the initial conditions of the reaction); (5) the spectra of the postulated transient intermediates are then modified until the residual spectrum is minimal and trendless.

Other Experimental Methods. The lactic acid dehydrogenase (LDH) competition experiment was carried out in the same stopped-flow apparatus in the fluorescence mode with excitation at 340 nm and emission measured using a (460 nm) GG400 band-pass filter. The experimental conditions were the same as those used in the kinetic absorbance experiments described above, with the addition of 20 μM LDH. Baseline enzyme and coenzyme fluorescence was subtracted from the kinetic traces. Fluorescence intensities were converted to micromolar concentrations using an NADH standard curve determined using the stopped-flow spectrophotometer in the same configuration and the same instrumental settings used in the kinetic measurements.

The pH-jump experiments on the csGDH-catalyzed reaction were carried out under the same final conditions used in the csGDH transient-state kinetic experiments described above. The method used was that previously described in our application of this technique to the blGDH-catalyzed reaction (*13*) as discussed in the text.

The determination of the K_D and enthalpy of formation of the csGDH−NADH and csGDH−NADH−L-glutamate complexes followed the approach previously described in our corresponding study of the blGDH−NADPH complex (*14*) with the exception of the use here of the Microcal Omega isothermal titration calorimeter instead of the LKB flow calorimeter used in the previous study. Titration curves were developed by stepwise addition of 4−8 μL of NADH solution (0.1 M potassium phosphate buffer, pH 7.6) into a stirred cell (400 rpm) containing 1.36 mL of 150 μM csGDH also in 0.1 M potassium phosphate buffer, pH 7.6 (*15*). Resultant curves were fit with sequential binding site models as described previously (*16*). Such calculated binding enthalpies were plotted versus temperature and fit to equations according to a single two-state equation as derived by Fisher (*17*) as well as by Eftink and Biltonen (*18*).

RESULTS AND DISCUSSION

Component Time Course of the csGDH Forward Reaction. The results and deconvolution of a multiwavelength transient time course study carried out at 0.25 ms and 1 nm intervals are shown in Figure 1. Figure 1A shows some selected spectra of the array at selected fixed points in time.

As noted in our previous paper (*5*), the analysis of such an array requires three successive steps: (1) the deconvolution of each observed fixed-time spectrum (such as those shown in Figure 1B) into individual components of determined shapes and extinction coefficients in such a way that the sum of their absorbance spectra at any point in time adds up quantitatively to the absorbance spectrum observed at that point in time, (2) the assignment of each resolved component to a known or a postulated intermediate enzyme form, and (3) the demonstration of the kinetic competence of the resulting time courses of each such resolved component to occupy its position in a postulated mechanism. We present here the results of the application of each of these steps to the oxidative deamination reaction catalyzed by csGDH. Procedures for accomplishing each of these steps are listed in the Materials and Methods section of this paper and are described in some detail in the previous paper in this series (*5*). Here, we will describe the results of such an analysis of the csGDH forward reaction and compare them with the corresponding component time courses of the blGDH reaction.

Resolution of Fixed-Time Transient Spectra. K_D values obtained from binding curves for the stable complexes of csGDH (ER and ERG) required for the development of model spectra (as described under Materials and Methods) are shown in Table 1. The spectroscopic characteristics of these complexes determined as described in the Materials and Methods section are also listed in Table 1 along with the previously published values of the corresponding blGDH complexes. Model spectra used in the deconvolution of the csGDH fixed-time spectra are shown in Figure 1B. The spectra of stable csGDH complexes are shown as solid lines, and those of two transient forms revealed by the deconvolution process are shown by dotted lines. The resolved spectrum is shown in Figure 1C. As can be seen from the small and quite trendless residuals shown in the bottom panel

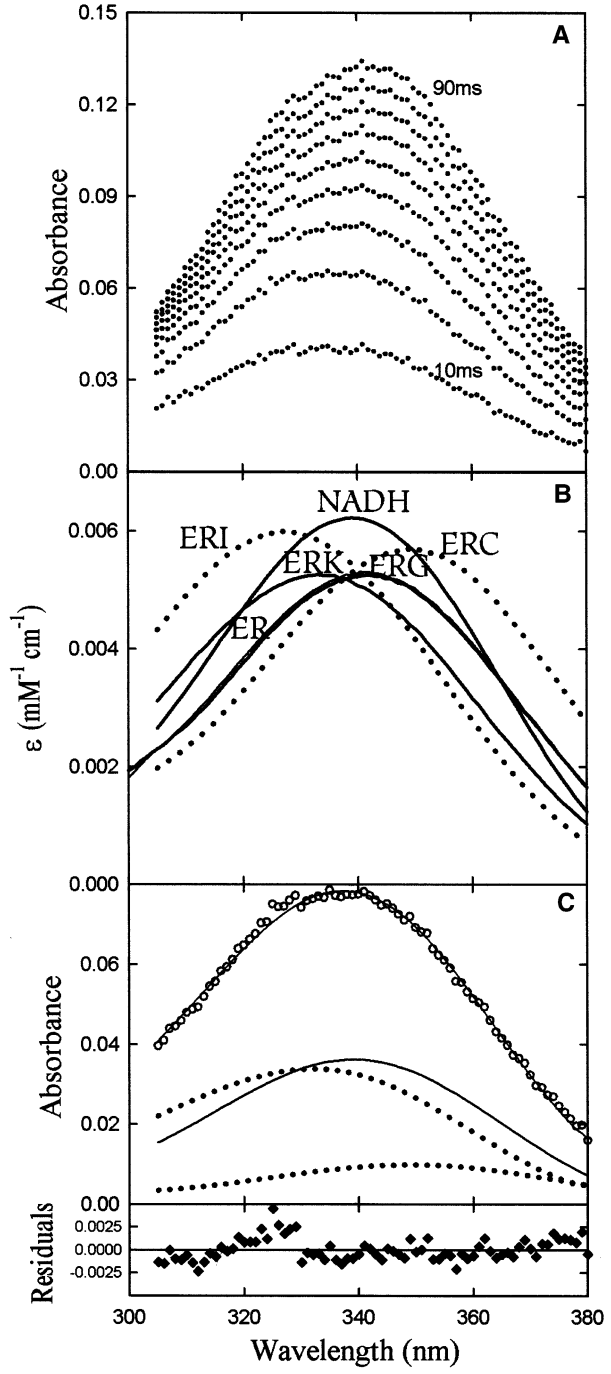

FIGURE 1: Resolution of fixed-time spectra of the csGDH oxidative deamination reaction. (A) Selected individual fixed-time spectra of the multiwavelength absorbance time course array collected at 0.25 ms intervals. Those shown here differ by 10 ms intervals from 10 to 90 ms. (B) Model component spectra used in the analysis. Spectra obtained by direct measure of stable complexes are indicated by solid lines. The ER and ERG spectra were obtained by spectrophotometric titrations of csGDH. The csGDH−ERK complex proved to be too unstable to provide a sufficiently accurate model spectrum. We have therefore used the directly determined blGDH−ERK spectrum (*5*) which appears to resemble that of the csGDH complex. Model spectra of the csGDH−ERI and csGDH−ERC complexes, formed by manipulation of a blGDH−ERK spectrum (*9*) and a csGDH−ERG spectrum, respectively, to fit the kinetic multiwavelength array (as described under Materials and Methods), are indicated by dotted lines. (C) Typical deconvolution of a spectrum of the csGDH reaction into components. Wavelength-dependent residuals representing the differences between the sum of the resolved component absorbances and the experimentally observed values are shown in the lower panel.

Table 1: Comparison of Models Determined Spectroscopically at pH 7.6, 25 °C, and 0.1 M Potassium Phosphate

	csGDH[a]			blGDH[b]		
	λ_{max}	ϵ (mM^{-1} cm^{-1})	K_D (μM)	λ_{max}	ϵ (mM^{-1} cm^{-1})	K_D (μM)
R[d]	340	6.22		340	6.22	
ER	342	5.24	9.0 ± 0.5[c]	343	5.14	23 ± 0.3 (10)
ERG	342	5.20	2.9 ± 0.2	343	5.47	0.13 ± 0.07 (26)
ERK	333	5.2		333	5.2	0.5 ± 0.1 (27)
ERC	349	5.2		349	5.7 (4)	
ERI	327	6		327	6 (4)	

[a] Experimental values from this work. [b] Previously published values. [c] Since model spectra have been derived at points on the binding curve at or above the K_D, the error in the estimation of free R is less than one-fourth the error of the K_D itself. [d] NADH or NADPH.

of the figure, the spectrum can be resolved using only three-component spectra. This three-component pattern was found to suffice throughout the 2−80 ms time range, which comprises the major portion of interconversions of central complexes. The components consist of a highly blue-shifted species ($\lambda_{max} = 327$), a highly red-shifted species ($\lambda_{max} = 349$), and an unshifted species ($\lambda_{max} = 340$). The ultra-blue-shifted entity is provisionally identified as ERI, based on its spectral similarity to that of the corresponding complex identified earlier in the blGDH reaction (*5*), and on its early occurrence in the csGDH time course. The ultra-red-shifted entity is similarly assigned to the later forming ERC complex on the same basis. The third component represented a spectrum indistinguishable from that of free NADH. No evidence of components corresponding to the previously established spectra of ER, ERK, or ERG was found at any point throughout the observed portion of the reaction time course.

Selected examples of an ordered series of these fixed-time spectral components for the csGDH-catalyzed α-L-glutamate reaction plotted vs time are shown by the open circles in Figure 2.[3]

Transient-State Kinetic Isotope Effects (tKIE's). Figure 3A shows the 340 nm time courses of the blGDH transient-state α-deuterio-L-glutamate reaction along with that of the corresponding α-protio-L-glutamate reaction. The transient-state kinetic isotope effect (tKIE) has been defined as

$$\mathrm{tKIE}(t) = \frac{\mathrm{d}[C^H]/\mathrm{d}t}{\mathrm{d}[C^D]/\mathrm{d}t}$$

where $[C^H]$ and $[C^D]$ may be either the concentrations of any component or the magnitude of a specific signal at a given point in time for the unsubstituted and the α-deuterio reactions, respectively. The tKIE time course of the A_{340}

[3] The probable error estimates for the rate constants listed in the legend to Figure 2 represent nothing more than the goodness of the fit of the reaction sequence of eq 6 to the set of experimentally determined component time courses shown in the figure. We ascribe no real significance to the values of any individual rate constant. A mathematical solution to a set of six differential equations can be provided with nearly equal accuracy by any of a very large number of sets of interactive numerical coefficients whose individual values may vary by orders of magnitude (*25*). Therefore, this particular numerical set only provides proof of the kinetic competence of the reaction scheme of eq 5 by showing that there exists at least one set of numbers that provides a reasonable fit to the data. (Attempts to fit alternative schemes to the data resulted in qualitatively worse fits.)

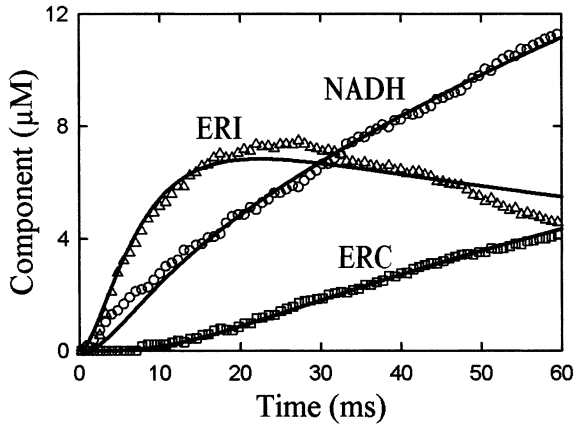

FIGURE 2: Spectroscopically resolved component concentrations of the csGDH reaction plotted vs time. Only three components (ERI, R, and ERC) were required and permitted by the analysis. The solid lines represent the best fit of eq 6 to the data using $k_1 = 160 \pm 36$, $k_2 = 16 \pm 60$, $k_3 = 110 \pm 23$, $k_4 = 400 \pm 70$, $k_5 = 320 \pm 18$, $k_6 = 900 \pm 72$, $k_7 = 140 \pm 3.0$, $k_8 = 3.4 \pm 0.2$, $k_9 = 87 \pm 3.0$, and $k_{10} = 170 \pm 5.0$.

signal is shown in Figure 3C. We have previously shown by a rigorous mathematical proof (*19*) that in any sequential reaction scheme the tKIE time course of any specific signal is governed by three absolute rules. Case 1: If *only* prehydride transfer species contribute significantly to that signal, then the tKIE will have a value of unity at $t = 0$ and will then decrease with time. Case 2: If *only* posthydride transfer species contribute significantly to the signal, then the tKIE will have the value of the intrinsic KIE (KIE_{int}) at $t = 0$ and will then decrease with time. Case 3: If *both* pre- and posthydride species contribute significantly to the signal, then the tKIE will have a value of unity at $t = 0$ and will rise to a maximum value $\leq KIE_{int}$ and then fall with increasing time. These rules are independent of the values of the KIE_{int} and of any rate constants involved in the kinetic expression of the reaction. We have found experimental evidence for the occurrence of all three cases (*19*, *20*). The tKIE shown in Figure 3C clearly shows a strict adherence to the case 2 criteria, proving that the A_{340} signal of the csGDH reaction contains contributions arising solely from posthydride transfer entities.

Nature of the Apparent Free NADH Species. A surprising feature of this set of component time courses is the apparent release of free NADH (R) at a very early stage of the mechanism. By inspection it would appear that this release point must follow the formation of the ERI complex and precede the formation of the ERC complex. Thus any mechanism that can account for this observed phenomenon must include an ERI $\rightleftharpoons$ EI + R step. Any of a number of very complicated overall mechanisms may then be invoked to account for the full set of component time courses. Any such mechanism, however, must contain the following feature:

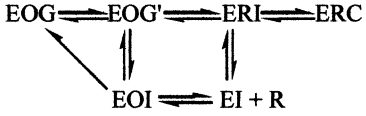

(4)

While such product "bleed-off" steps and the futile cycles to which they lead are not unknown in enzyme-catalyzed reactions, the reaction scheme of eq 4 appeared to us to be

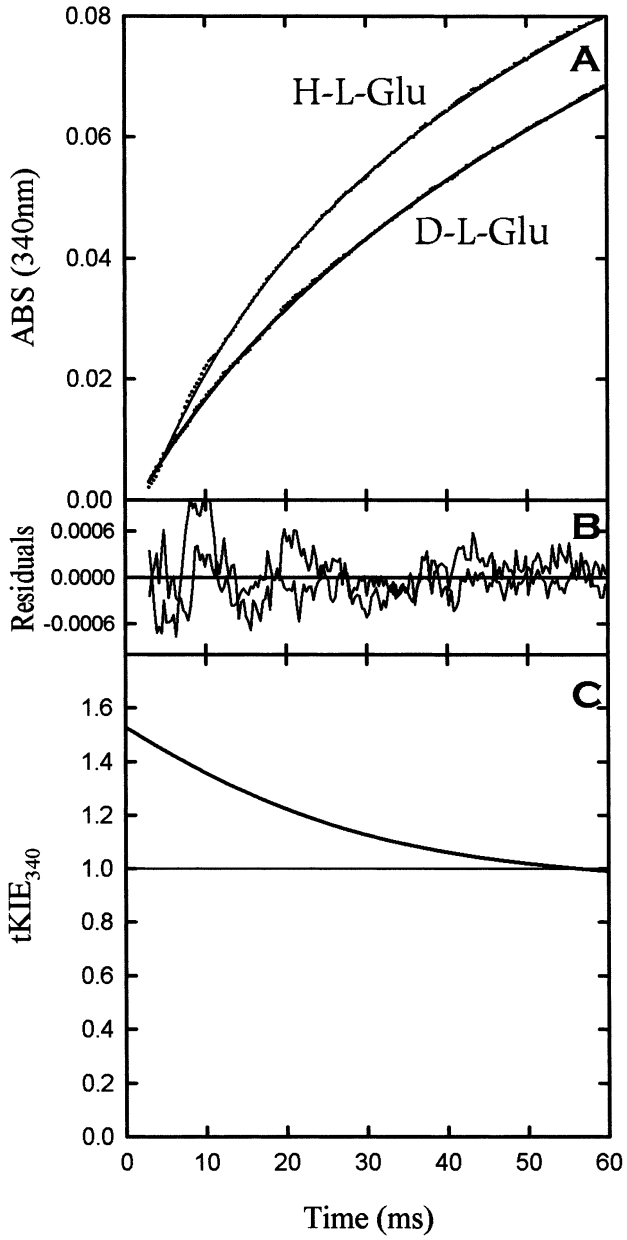

FIGURE 3: Transient-state kinetic isotope effect of the csGDH oxidative deamination reaction. (A) The experimental points represent the 340 nm time courses of the unsubstituted and the α-deuterio-L-glutamate reactions. The solid lines fitted to each data set are solutions to a standard two exponential equation and are used solely to provide smoothed curves which are then numerically differentiated to provide dA_{340}/dt vs t curves. The lower panel shows the differences between the data and the fitted curve. (C) tKIE of A_{340} vs time, calculated from the ratio of the dA_{340}/dt values of the smoothed curves, as defined by eq 3 in the text.

quite unlikely on the basis of chemical, physical, and metabolic grounds. An alternative possibility would be that the unshifted "R" component represents some ER complex rather than free NADH. To test this possibility, we ran the reaction in the presence and in the absence of pig heart lactic dehydrogenase (LDH), which reacts quickly with NADH to form a tight binary complex whose 340 nm excited fluorescence is at least 2.5 times that of free NADH. As can be seen from the corresponding fluorescence traces in Figure 4, no evidence of such an LDH−NADH complex appears for the first 40 ms of the reaction. Evidence of the ultimate appearance of free NADH does appear later in the time

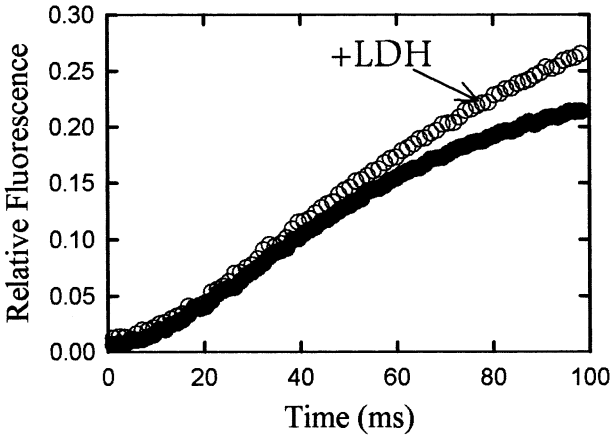

FIGURE 4: Effect of lactic dehydrogenase on the csGDH time course. The closed circles represent the relative 340 nm excited fluorescence of the reaction in the absence of lactic acid dehydrogenase, while the open circles represent the signal from an identical reaction with the added presence of 20 μM lactic acid dehydrogenase.

course, but only at a time significantly later than that of the accumulation of substantial concentrations of both ERI and ERC which presumably precede its release. The reaction scheme of eq 4 is thus ruled out and must be replaced by the scheme:

$$\mathrm{EOG} \rightleftharpoons \mathrm{ERI} \rightleftharpoons \mathrm{ERX} \rightleftharpoons \mathrm{ERC} \overset{\mathrm{H^+}}{\rightleftharpoons} \mathrm{ERK} \rightleftharpoons \mathrm{E + K + R} \quad (5)$$

where "ERX " designates one or more reduced coenzyme complexes in which the R spectrum is unshifted.

We now must face the question: what is the nature of this ERX complex? The most logical explanation for such a complex having a totally unshifted NADH spectrum is to ascribe it to a ternary complex in which the enzyme is in its open conformation, with the bound coenzyme in contact with the solvent. It is well established that spectral shifts can be induced by changes in the polarizability of the chromophore. The practical measure of this effect is the change in the refractive index in the immediate vicinity of the chromophore. Since such effects decrease with the third power of the distance, only the first layer of atoms surrounding the chromophore will have any significant influence. Thus, the open conformation of the complex leaves the chromophore largely surrounded by solvent water, resulting in no significant shift in its spectrum. In the closed conformation, on the other hand, this aqueous environment is replaced by protein (whose refractive index is much higher than that of water), and as shown by X-ray crystal structures, any one of several functional groups of varying electronic structure may engage in an induced dipole interaction with the chromophore, resulting in a substantial shift in λ_{max}. It may be noted that while closed forms of the various E−R−ligand complexes may exhibit distinctive spectral shifts, all open complexes, being unshifted, are indistinguishable from another.

Test of Kinetic Competence of the Proposed Mechanism. On the basis of this hypothesis, we now proceed to establish a more reasonable set of kinetically competent reaction-

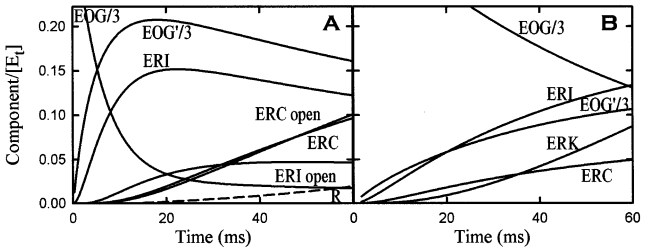

FIGURE 5: Comparison of the time courses of the individual components of the csGDH- and blGDH-catalyzed reactions. (A) Components of the csGDH reaction. These curves were calculated using the individual rate constants listed in the legend to the fitted curve shown in Figure 2. The time course of the release of free R has been calculated from the difference between the fluorescence of the csGDH time courses in the presence and in the absence of LDH. The data have been adjusted for an estimated lag time averaging 3 ± 2 ms for the R + LDH ⇌ LDH−R reaction. (B) Components of the blGDH reaction. These curves are modified versions of those shown in ref *5*.

component time courses. In doing so, the inability to distinguish between the various open complexes would appear to be a severe liability. Fortunately, however, since closed complexes may be expected to intervene in the reaction sequence between pairs of open complexes, we can largely replace spectral resolution with kinetic resolution. The best fit to the component time courses is shown by the solid lines in Figure 2, based upon the following reaction sequence:

$$\mathrm{EOG} \underset{k2}{\overset{k1}{\rightleftharpoons}} \boxed{\mathrm{EOG}} \underset{k4}{\overset{k3}{\rightleftharpoons}} \boxed{\mathrm{ERI}} \underset{k6}{\overset{k5}{\rightleftharpoons}} \mathrm{ERI} \underset{k8}{\overset{k7}{\rightleftharpoons}} \mathrm{ERC} \underset{k10}{\overset{k9}{\rightleftharpoons}} \boxed{\mathrm{ERC}} \quad (6)$$

where the boxed complexes indicate spectrally shifted (and, thereby, closed) enzyme forms, and the unboxed complexes indicate spectrally unshifted (and, thereby, open) enzyme forms.

It may be noted that, while the data from the LDH effect (Figure 4) are not used directly in the kinetic fitting operation, our solution is quite compatible with those results; free NADH is released only at a relatively late stage in the reaction. The remainder of the free NADH (R) component at any point in time must then represent the sum of ER−ligand complexes having open (and, thereby, spectrally unshifted) conformations. To obtain a kinetically competent fit to the component time course, it was necessary to assume the presence of a smaller and somewhat more slowly converting amount of an open ERI complex as well as an open form of ERC nearly equal to, and rapidly equilibrating with, the closed ultra-red-shifted closed form. The solution also required the slow formation of a closed form of an ERK complex whose spectrum is indistinguishable from that of the closed form of ERI. In panel A of Figure 5, we show the resolved component time courses of the csGDH reaction from the fit shown in Figure 2, based on the reaction scheme of eq 6. The time course of the release of free R shown by the dashed line in Figure 5A is based on data calculated from the LDH experiment shown in Figure 4. This R release step logically must be preceded by the formation of an ERK complex. No such entity is observed in the blGDH reaction, whose ERK complex must be presumed to have a very large forward commitment factor.

Comparison of the csGDH and blGDH Component Time Courses. In panel B of Figure 5 we show a previously published set of resolved component time courses for the corresponding reaction catalyzed by the mammalian form of the enzyme, blGDH (*5*). Comparing the two reactions, it can be seen that while the same complexes are formed in the same sequential order (albeit at a 5-fold slower rate and with a more pronounced accumulation of the ERK complex in the blGDH case), the principal difference in the two forms is the total absence of significant concentrations of any of the open forms of the posthydride complexes observed in the csGDH reaction. The absence of such forms in the spectra does not in any way imply that such forms are not integral parts of the blGDH reaction. We know, for example, that there must be an open form to permit the previously observed prehydride proton release and the posthydride release of ammonia. The absence of such forms means only that in the blGDH reaction each open form must have very large forward and reverse commitment factors.

Comparing the phenomenological detail of Figure 5 with the single-wavelength time courses shown in Figures 3 and 4, it is apparent that the multiwavelength, resolved component time course approach demonstrated here and in ref *5* provides a substantial increase in our ability to obtain direct real-time resolution of the sequence of steps in an enzyme-catalyzed reaction.

Structural Evidence of Open and Closed Forms of Pyridine Nucleotide Linked Dehydrogenases. The concept of relative domain motions leading to conformations in which the active site of an enzyme may be alternatively open or closed is a generally accepted one. In the case at hand, crystal structures of both an open enzyme−NAD form and of two slightly different enzyme−L-glutamate closed forms have been reported (*4*, *21*). Substantial variations in the degree of closure of forms of GDH from a variety of organisms have been noted. While crystallographic structures by their nature represent isolated static forms, dynamic evidence on this point has been provided by the recently published work of Nakasako et al. (*22*), who used small-angle X-ray scattering to demonstrate the occurrence of spontaneous relative domain motions of a bacterial GDH molecule in solution. These studies, which focused on the tightly bound hydration water molecules in the active site cleft, demonstrated the existence of a dynamic set of variations between an open, a partially closed, and a fully closed form on the various subunits of any given GDH hexamer.

Thermodynamic Evidence of Differences in the Conformational States of csGDH and blGDH. Direct isothermal calorimetric measurements of the $\Delta H°$ of binding of NADH to csGDH at various temperatures are shown by the open circles in Figure 6. Corresponding data for the $\Delta H°$ of binding of NADPH to blGDH are plotted as filled circles in Figure 6. While the data indicate a substantial negative heat capacity (ΔC_p) in both reactions, it can be seen that the csGDH data represent a distinct concave *upward* trend, while those for blGDH show an opposite concave *downward* shape. It had been observed previously that the binding of a ligand to a protein generally produces a substantial negative ΔC_p of 200−600 cal deg^{-1} mol^{-1} (*16*). While a number of theories had been advanced to account for this phenomenon, most of these studies involved ΔC_p's calculated from $\Delta H°$ values obtained at only two temperatures typically covering only a

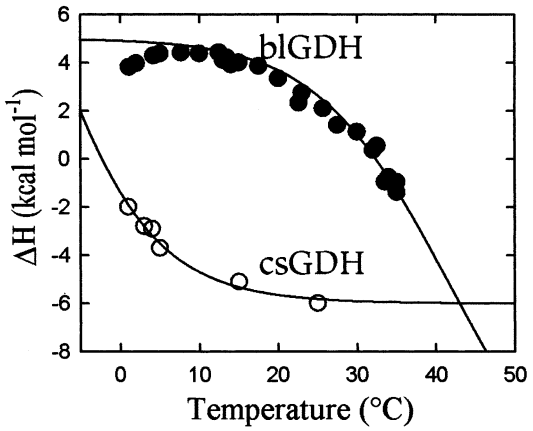

FIGURE 6: Comparison of the temperature dependence of the enthalpy of formation of the ER complexes of csGDH and blGDH. The data were obtained from isothermal calorimetric titrations as described in the Materials and Methods section. The solid lines were calculated using the single two-state equation (eq 8), based on the mandatory binding scheme shown in eq 7. csGDH: $T_0 = -5$ °C, $\Delta H_0 = 22$ kcal mol^{-1}, and $\Delta H_B = -5.7$ kcal mol^{-1}. blGDH: $T_0 = 46.2$ °C, $\Delta H_0 = 22$ kcal mol^{-1}, and $\Delta H_B = -16.8$ kcal mol^{-1} (data from ref *14*).

10° span. The data shown by the filled circles in Figure 6 represent the first fine-grained study over an extended range comprising (in a later extension) an array of $\Delta H°$ values at 35 separate temperatures over a range of 38 °C. Earlier theories of the physical basis of ΔC_p's of binding were inadequate to explain data such as those shown in Figure 6. We were, however, able to account for the thermal behavior of this binding reaction (as well as the widely different variations of it in other related binding reactions) with considerable accuracy on the basis of a very simple theory. We need only to assume that an enzyme exists as an equilibrium mixture of two conformations, only one of which can bind the ligand as shown in the equation:

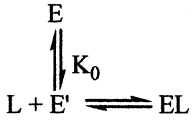

(7)

The temperature dependence of the observed enthalpy of binding (ΔH) of such a system measured at saturating concentrations of L is

$$\Delta H = \Delta H_B\left(\frac{\Delta H_0}{1 + K_0}\right) \tag{8}$$

where $K_0 = e^{\Delta H_0((T-T_0)/RTT_0)}$ is the temperature-dependent equilibrium constant of the E ⇌ E′ reaction, ΔH_B is the enthalpy of binding of the ligand to the E′ form of the enzyme, ΔH_0 is the enthalpy of the isomerization step, and T_0 is that temperature at which $K_0 = 1$. The behavior of such a system is shown in Figure 7. A very similar theory has been developed by Eftink and Biltonen (*18*).

We have shown that the observed data for all pyridine nucleotide dehydrogenase binding reactions (and for that of several other enzymes, as well) can be fitted very closely by this simple equation with only two variable constants, T_0 and ΔH_B, and an unvarying value of 22 ± 2 kcal mol^{-1} for ΔH_0 (*17*).

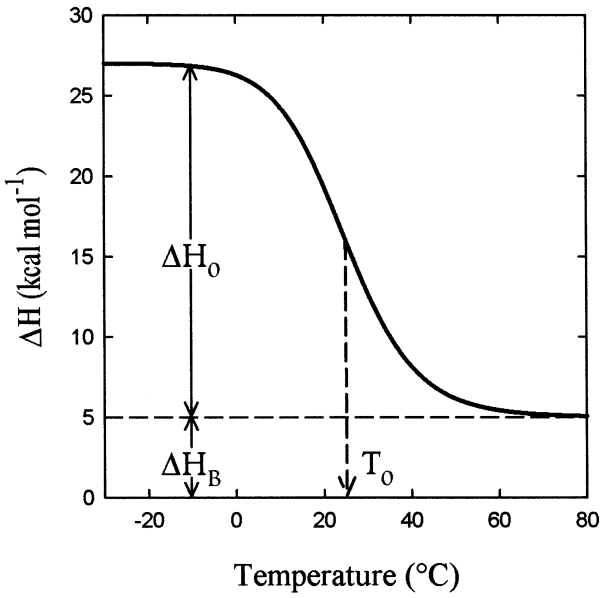

FIGURE 7: Theoretical curve for the temperature dependence of the enthalpy of the mandatory binding of a ligand to one form of an enzyme that exists as an equilibrium mixture of two forms as defined in eq 7 for the case where $T_0 = 20$ °C, $\Delta H_0 = 22$ kcal mol^{-1}, and $\Delta H_B = 5$ kcal mol^{-1}.

The solid lines in Figure 6 represent the fit of eq 8 to the ΔH of E−R binding for both csGDH and blGDH. The parameters found for csGDH are $T_0 = -15°$ and $\Delta H°_B = -5.7$ kcal mol^{-1}. The upward-concave shape of the data over the observable range indicates that the state of the free enzyme in this case lies at the extreme right-hand side of the theoretical curve in Figure 7 and is predominately in the high-enthalpy E′ state. The fit of eq 8 to the corresponding $\Delta H°$ of binding data of the blGDH−R reaction shown by the solid line in Figure 6 produces parameters of $T_0 = +43$ °C and $\Delta H_B = 5$ kcal mol^{-1}. In contrast to the temperature dependence of the csGDH case in Figure 6, the downward-concave shape of the data shows that the state of the free form of blGDH occupies the left-hand region of the theoretical curve in Figure 7 and must be predominately in the low-enthalpy state at experimentally accessible temperatures. The thermodynamic properties of such E ⇌ E′ two-state transitions suggest that they represent the interconversion of closed-to-open active site forms. As such, they would correspond to limited portions of the general process of the unfolding of a protein. The large positive enthalpy (>150 kcal/subunit) accompanied by large positive entropy changes is usually ascribed to the increased area of solvation of hydrophobic residues in the unfolding process. On this basis, the E ⇌ E′ transition would involve the exposure of roughly 15% of the buried residues in a protein. This interpretation is supported by the surprising commonality of a +22 kcal mol^{-1} $\Delta H°_0$ among a number of quite diverse enzymes and by the substantial decrease in thermal stability of forms with subzero T_0 values (*17*). The most convincing supporting evidence on this point, however, is the small-angle X-ray study of Nakasako et al. of the changes in hydration accompanying domain motions in open and closed conformations of a bacterial GDH, to which we have referred in a previous section (*22*). These authors demonstrated the existence of three conformations of a GDH active site cleft, one completely closed, one partially closed, and one completely open, showing increasing hydration of cleft surface with the degree of opening. It may be presumed that these three states of closure correspond in some way with the open, partially closed, and more fully closed forms of a closely related bacterial GDH identified in the X-ray crystallographic studies of the Sheffield group (*4*). Due to its location in the exponential term of K_0 in eq 8, T_0 is a very sensitive function of K_0. Indeed, we have observed T_0 values varying from −25 to +45 °C among various dehydrogenase complexes (*17*). A particular point of interest is the 23 °C T_0 value of the blGDH−EGR complex. Unlike the other two forms of blGDH, which have T_0 values either above or well below the experimental range, the E−G complex is equally distributed between open and closed forms between 15 and 25 °C. It would seem likely, therefore, that the species involved in the csGDH EG + R ⇌ EGR reaction from the calorimetric data reported here is in fact the partially closed form identified structurally by both conventional X-ray structures and small-angle X-ray hydration findings. Thus, it is clear that the degree of cleft closure of csGDH is a sensitive function of the nature of its ligand in any given complex. Therefore, it is to be anticipated that, at any fixed pH and temperature, the enzyme will change from open to closed forms and back as the reaction proceeds from one complex to the succeeding ones, just as our multiwavelength transient-state studies have suggested.

Differences in the Location of Active Site Cleft-Opening Steps along the Reaction Time Courses of the csGDH and blGDH Reactions. Important as this finding is in proving that there is indeed a facile and structurally relatable cleft-opening process occurring in GDH in solution, we still require evidence of the kinetic competence and mechanistic locus of these events. To establish this necessary relationship between structural phenomena and the kinetically located spectrally unshifted forms to which we ascribe those phenomena in the csGDH reaction, we turn to a "pH-jump" technique which we have successfully applied to the blGDH reaction (*13*). In this approach, a transient-state reaction run at an initial pH solution is subjected to abrupt jumps in pH at various points along its time course. The basis of interpreting the results of such an experiment is the fact that pH jumps can affect only enzyme complexes that exist in their active site open form at the specific point in time of a given jump. While the method is described in some detail in a previous paper (*13*), it essentially involves a sequence of three experiments: (1) A stopped-flow reaction is initiated by mixing one weakly buffered solution containing enzyme and NAD with a solution containing enzyme and L-glutamate in the same buffer. At various points in time after the onset of the reaction, the pH of the mixed solution is raised by inducing a second mixing event to suddenly jump the reacting solution to a higher pH. (2) A control experiment (an "iso-pH" jump) in which the second mixing solution is at the original pH is carried out to correct for the dilution effect of the pH jump. (3) A single mixing experiment at the final pH of the pH-jumped solution is carried out in order to assess the maximum effect that the pH jump could have caused if the active site was fully accessible to the solvent. From these three values, fractional rates, designated as F_r, are calculated as $F_r = V_{(6.2+8.5)} - V_{(6.2+6.2)}/V_{(6.2+8.5)}$. The results of such an experiment on the csGDH reaction are shown in panel A of Figure 8. It can be seen that the production of

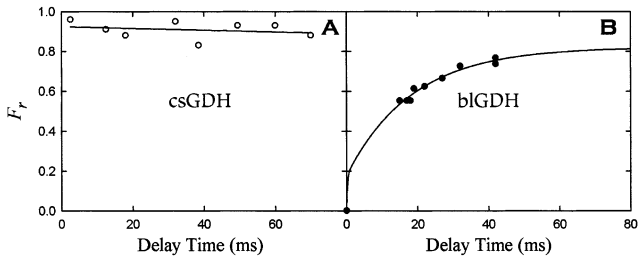

FIGURE 8: Comparison of the results of pH-jump experiments on csGDH- and blGDH-catalyzed reactions. The ordinate values indicate the fraction of the enzyme forms whose active sites are open to the solvent. F_r is defined in the text.

reduced coenzyme complexes remains constant at an amount of about 90% throughout the csGDH reaction time course. While this result may appear to provide little detailed information, when considered in terms of the changing distribution of enzyme complexes during the reaction time course, this constant value leads to some quite specific conclusions. Referring to Figure 5A, we note that, in the initial part of the time course, EOG complexes comprise the bulk of the enzyme forms. Thus, we conclude that any EOG complexes are 90% in open forms. As time passes, however, EOG drops progressively and by 70 ms it accounts for only 50% of the total enzyme. The constant value of 90% open forms, then, must be accounted for by a corresponding increase in open forms of ERI and ERC. Indeed, it can be seen by inspection that, throughout the time course, the sum of 90% of [EOG] plus that of the open forms of [ERI] and [ERC] remains at the constant value of 90%. It may be noted that both ERI and ERC are each in approximately 50% open forms. This result confirms the assignment of the early portion of the unshifted spectral component as being due to open forms of enzyme-reduced coenzyme complexes.

By way of comparison, we present the results of a corresponding pH-jump experiment on the blGDH reaction in panel B of Figure 8. It can be seen that the pH-jump patterns of the two GDH reactions are strikingly different. Figure 8B shows that only a small fraction (<10%) of the active sites of blGDH are open to the solvent initially as predicted by the isothermal calorimetric titration data shown in Figure 6.[4] This fraction increases proportionally to [EOG], reaching a value of 35% only after some 50 ms, a point where the open form of EOG has reached a maximum. There is no evidence of any substantial accumulation of open ERI or ERC complexes, even though it must be assumed that such forms must exist at least momentarily.

Thus, in the component time courses of each enzyme, the assignments of spectroscopically distinguishable components to either open or closed kinetically competent chemically defined species agree with the corresponding thermodynamic, structural, and solvent accessibility evidence. A reason for the strikingly different transient-state kinetic patterns of two

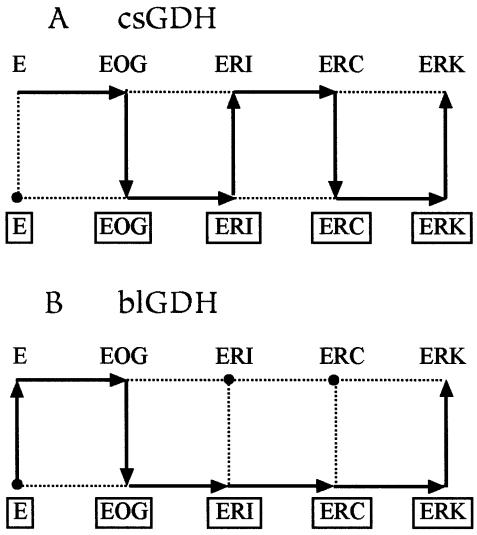

FIGURE 9: Conformational time courses of the catalytic reactions. The boxed complexes indicate reactive forms in which the active site is closed to the solvent, while the unboxed complexes are presumed to be open forms. (A) The csGDH-catalyzed reaction. (B) The blGDH-catalyzed reaction.

enzymes having nearly identical active site functional group geometries has now become clear. The csGDH reaction begins with both the apoenzyme and its prehydride transfer complexes predominately in the open form, while the posthydride complexes are roughly evenly divided between alternating open and closed forms. The blGDH reaction, on the other hand, begins with largely closed forms, and the closed form continues to predominate throughout the posthydride phases of the reaction, opening only briefly for required product release, substrate addition, and related steps.

A comparison of our current understanding of the occurrence and mechanistic location of kinetically significant domain movements in the mechanisms of the reactions catalyzed by csGDH and blGDH, respectively, is shown in panels A and B of Figure 9, in which the closed forms of each enzyme complex are located on the lower line of each scheme, while the corresponding open forms are located on the upper line. The solid lines indicate our current state of knowledge of the course of each reaction as the state of the active site cleft changes during the succession of chemical steps. It is important to note that these are both minimal schemes including only features required to explain our observed experimental results. Thus, the depiction of the later portion of the blGDH reaction as proceeding strictly through a series of closed enzyme forms is not to be taken literally—it is certainly possible (if not probable) that one or more of these steps does involve passage through on open enzyme form such as those prevalent in the csGDH reaction. The implication of the sequence as drawn in panel B of Figure 9[5] is only that, where such unnoted extra open enzyme forms

[4] The nature of eq 7 is such that a negative slope of the dependence of ΔH on temperature is ascribed to the properties of the reactant form of the E ⇌ E′ equilibrium shown in Figure 7, regardless of the algebraic sign of ΔH_0 itself (*17*). As shown in Figure 6, at 5 °C (the temperature of the csGDH kinetic experiments) ΔH is only about 1 kcal mol^{-1} above ΔH_B, indicating that about 95% of free enzyme is in the high-enthalpy E′ form, while the fraction of blGDH in the high-enthalpy form at that temperature is less than 10%. The agreement between the calorimetric and pH-jump results adds further weight to the assignment of E and E′ forms as being closed and open, respectively.

[5] The reaction coordinate schemes shown in Figure 9 may be viewed as composites of two component reaction courses, one representing the multiple conformational changes in the protein as the reaction proceeds and a second reaction course reflecting the ability of each conformation to participate chemically in the succeeding step. Because of the possibility of minor species reactivity, these two time courses are not necessarily congruent. Indeed, it is precisely such differences in synchronization of the chemical and energetic time courses that permit such features as the transduction of ligand binding energy into a catalytic driving force as we have described in ref 21.

do occur, they do not accumulate in measurable amounts in the blGDH reaction. Consequently, while mechanistically important, such complexes cannot be kinetically significant.

CONCLUSIONS

The concept of a ligand-induced domain movement in enzymatic catalysis is an old one, dating back at least to Koshland's "induced fit" hypothesis and elaborated for multisubunit proteins in the various theories of allosteric behavior. More pertinent to our specific case, a "conformational change" has been frequently invoked in pyridine nucleotide dehydrogenase mechanisms. Such events are usually based on the observance of a transient-state kinetic burst (which actually signifies only the presence of a ligand concentration-independent step) and are typically singular in nature. The demonstration presented here, of an entire pattern of physically observed and mechanistically located domain-shifting events, and the striking variance of such patterns in two highly homologous enzymes may imply some consequences applicable to the current concepts of enzyme mechanisms in general.[6] In a previous paper (*24*) we presented evidence for the phenomenon of the transduction of substrate binding energy into later catalytic steps in the blGDH-catalyzed reaction. The energetic linking device in that process was very similar to the domain-shifting events whose occurrence and mechanistic location we have described here. This agreement and newly added evidentiary detail suggest that the picture of the enzyme as a mechanically reciprocating chemical machine may now be given some degree of credence.

It would seem unlikely that the pattern of phenomena observed here should be unique to GDH. Indeed, our thermodynamic studies of the pyridine nucleotide linked dehydrogenases showed that the complexes of every member of that class involved an $E \rightleftharpoons E'$ transition having a $\Delta H°$ of 22 kcal mol^{-1} but with equilibrium constants that vary over 3 orders of magnitude between the various complexes of a given enzyme as well as between corresponding forms of different members of the class. Since it is unlikely that such behavior patterns would be unique to one particular class of enzymes, we suggest that domain-shifting phenomena of the type we have described here must now be considered as integral parts of the mechanisms of enzyme-catalyzed reactions.

[6] In a study of the kinetics of binding of α-ketoglutarate and NADH to csGDH, Basso et al. (*22*) concluded that the two ligands appeared to bind to different forms of the enzyme. They suggested that ternary complex formation may involve "the oscillation of the free, binary, and ternary glutamate dehydrogenase complexes between two different conformational states, termed E_1 and E_2". Interpreting E_1 and E_2 as representing the open and closed enzyme forms described here, their results add additional support for the catalytic mechanism we propose.

ACKNOWLEDGMENT

We thank Drs. Paul Engel and X. G. Wang for providing the *E. coli* clone and Dr. David Rice for prepublication release of csGDH X-ray crystallographic structures.

REFERENCES

1. Brunhuber, N. M., and Blanchard, J. S. (1994) *Crit. Rev. Biochem. Mol. Biol. 29*, 415−467.
2. Rife, J. E., and Cleland, W. W. (1980) *Biochemistry 19*, 2328−2333.
3. Baker, P. J., Britton, K. L., Engel, P. C., Farrants, G. W., Lilley, K. S., Rice, D. W., and Stillman, T. J. (1992) *Proteins 12*, 75−86.
4. Stillman, T. J., Baker, P. J., Britton, K. L., and Rice, D. W. (1993) *J. Mol. Biol. 234*, 1131−1139.
5. Maniscalco, S. J., Saha, S. K., and Fisher, H. F. (1998) *Biochemistry 37*, 14585−14590.
6. Saha, S. K., Maniscalco, S. J., Singh, N., and Fisher, H. F. (1994) *J. Biol. Chem. 269*, 29592−29597.
7. Maniscalco, S. J., Saha, S. K., Vicedomine, P., and Fisher, H. F. (1996) *Biochemistry 35*, 89−94.
8. Brunhuber, N. M. W., Thoden, J. B., Blanchard J. S., and Vanhooke, J. L., (2000) *Biochemistry 39*, 9174−9187.
9. Rice, D. W., Hornby, D. P., and Engel, P. C. (1985) *J. Mol. Biol. 181*, 147−149.
10. Fisher, H. F. (1973) *Adv. Enzymol. 39*, 369−417.
11. Fisher, H. F., Maniscalco, S., Wolfe, C., and Srinivasan, R. (1986) *Biochemistry 25*, 2910−2915.
12. Tinoco, I., Jr. (1960) *J. Am. Chem. Soc. 82*, 4785.
13. Saha, S. K., and Fisher, H. F. (1999) *Biochim. Biophys. Acta 1431*, 261−265.
14. Fisher, H. F., and Stickel, D. C. (1980) *FEBS Lett. 113*, 11−14.
15. Wiseman, T., Williston, S., Brandts, J. F., and Lin, L.-N (1989) *Anal. Biochem. 179*, 131−137.
16. Fisher, H. F., and Singh, N. (1995) *Methods Enzymol. 259*, 194−221.
17. Fisher, H. F. (1988) *Adv. Enzymol. Relat. Areas Mol. Biol. 61*, 1−46.
18. Eftink, M. R., and Biltonen, R. L. (1980) in *Biological Microcalorimetry* (Breezer, A. E., Ed.) pp 343−408, Academic Press, New York.
19. Fisher, H. F., and Saha, S. K. (1996) *Biochemistry 35*, 83−88.
20. Maniscalco, S. J., Saha, S. K., Vicedomine, P., and Fisher, H. F. (1996) *Biochemistry 35*, 89−94.
21. Stillman, T. J., Baker, P. J., Britton, K. L., Rice, D. W., and Rodgers, H. F. (1992) *J. Mol. Biol. 224*, 1181−1184.
22. Nakasako, M., Fujisawa, T., Adachi, S., Kudo, T., and Higuchi, S. (2001) *Biochemistry 40*, 3069−3079.
23. Basso, L. A., Engel, P. C., and Walmsley, A. R. (1995) *Eur. J. Biochem. 234*, 603−615.
24. Fisher, H. F., and Singh, N. (1991) *FEBS Lett. 294*, 1−5.
25. Moore, J. W. (1981) *Kinetics and Mechanism*, pp 218−323, John Wiley & Sons, New York.
26. Fisher, H. F., Adija, D. L., and Cross, D. G. (1969) *Biochemistry 8*, 4424−4431.
27. Cross, D. G. (1972) *J. Biol. Chem. 247*, 784−789.

BI0202068